INTERNATIONAL JOURNAL OF ROBUST AND NONLINEAR CONTROL
Int. J. Robust Nonlinear Control **9**, 799–815 (1999)

A NOVEL ANALYSIS AND DESIGN OF A NEURAL NETWORK ASSISTED NONLINEAR CONTROLLER FOR A BIOREACTOR

MEHMET ONDER EFE[1], ENDER ABADOGLU[2] AND OKYAY KAYNAK[3]*

[1] *Bogazici University, Electrical and Electronic Eng. Dept., Bebek, 80815, Istanbul, Turkey*
[2] *Bogazici University, Mathematics Dept., Bebek, 80815, Istanbul, Turkey*
[3] *Chair of Electrical and Electronic Engineering Department, Bogazici University, Bebek, 80815, Istanbul, Turkey*

SUMMARY

A novel approach is presented for the analysis and the design of a controller for a bioreactor. It is based on the model reference control theory, assisted by a neural network identifier. The control objectives specified in the paper require the controller to be a nonlinear one, however, it is shown that it is stable in the sense of bounded input bounded output and locally stabilizing in the sense of Lyapunov. The feasibility and the efficacy of the proposed approach are tested on the benchmark problem. Copyright © 1999 John Wiley & Sons, Ltd.

Key words: bioreactor control; model reference control; neural network identifier; bioreactor benchmark problem

INTRODUCTION

Chemical systems are often highly nonlinear and difficult to control. Nonlinearities may be intrinsic to the physics or a chemistry of a process or may arise through the close coupling of a number of simpler processes. In either case, complicated differential or difference equations of the system dynamics pose a challenging problem in the sense of mathematical tractability. This problem can somewhat be alleviated by using a simplified model, but a control approach designed on the basis of such a simplified model is unlikely to result in a satisfactory performance. A prime example is a bioreactor. The commonly used model for this process has few state variables but the controller design is highly involved due to the nonlinear characteristics of the process and the existence of limit cycles in the uncontrolled dynamics. Anderson and Miller[1] list

This paper was submitted for publication by editor M. D. Di Benedetto

* Correspondence to: Okyay Kaynak, Electrical and Electronic Engineering Department, Bogazici University, Bebek, 80815, Istanbul, Turkey.

Contract/grant sponsor: Foundation for Promotion of Advanced Automation Technology
Contract/grant sponsor: Bogazici University Research Fund
Contract/grant number: 97A0202

CCC 1049-8923/99/110799–17$17.50
Copyright © 1999 John Wiley & Sons, Ltd.
Received 31 July 1998
Accepted 11 May 1999

this plant as a challenging control problem and Agrawal and Lim[2] give an analysis of various control schemes.

In recent years tremendous advances have been made in technology and this has affected the practice of control engineering. With the advances in high speed computing, it is now possible and economically feasible to use complex, model-based control paradigms in practical applications, using advanced strategies derived from adaptive, nonlinear, and robust control theories. The problem of bioreactor control has also benefited from these developments and various novel (mainly adaptive) strategies, which have been reported in the literature,[3] with the objective of maintaining the process output close to the desired value in the presence of various uncertainties, including external disturbances, time-varying parameters, and unmodeled dynamics. A recent survey and comparison of various control configurations can be found in the paper of Zhao and Skogestad.[4]

A more recent tendency in process control is the blending of algorithmic techniques with other elements, such as logic, reasoning and heuristics. Such systems have come to be known as intelligent control systems.[5,6] A host of new control approaches are being used in this respect, based on fuzzy logic, neural networks, evolutionary computing and other techniques adapted from artificial intelligence. In demonstrating the feasibility and efficacy of such approaches in the control of nonlinear processes, bioreactor control has been taken as a case study by many authors,[7–9] some have addressed the topic directly. For example Feldkamp and Puskorius[10] take the bioreactor benchmark problem set by Ungar[11] and apply dynamic gradient methods, using neural networks for identification and control. In the work of Gorinevsky,[12] the same benchmark problem is treated using affine radial basis function network architecture. It is shown that a completely adaptive control of this strongly nonlinear system can be achieved with minimal *a priori* knowledge of its dynamics.

The approach used in this paper is different than those reported in the literature in that it is based on the well-known model reference control (MRC) technique, assisted by a neural identifier. The organization of the paper is as follows. Firstly, the bioreactor benchmark problem is described together with the equations governing the process dynamics. The following section introduces the MRC philosophy and continues with the selection of a special reference model for its application to the problem in hand. The philosophy that lies behind this specific choice is explained. An analysis of the whole system is then presented and the controller structure required for model following performance is established. The stability of the overall control is then elaborated upon, utilizing Lyapunov stability theorems. The paper continues with an explanation of how neural networks can be injected into the proposed rule of control. A brief explanation of neurocomputing is given and the partial identification scheme is scrutinized. Lastly the error dynamics is analysed and the effect of approximation error caused by the neural identifier is considered in the sense of output tracking capability. Conclusions constitute the last part of the paper.

PLANT MODEL

The model used is in this paper for the bioreactor is the one set by Ungar[11] as a benchmark problem. The process is a tank containing water, nutrients, and biological cells as shown in Figure 1. Nutrients and cells are introduced into the tank where the cells mix with nutrients. The cell concentration $c_1(t)$ and the amount of nutrients $c_2(t)$ per unit volume characterize the state of this process. The volume in the tank is maintained at a constant level by removing tank contents

Copyright © 1999 John Wiley & Sons, Ltd.

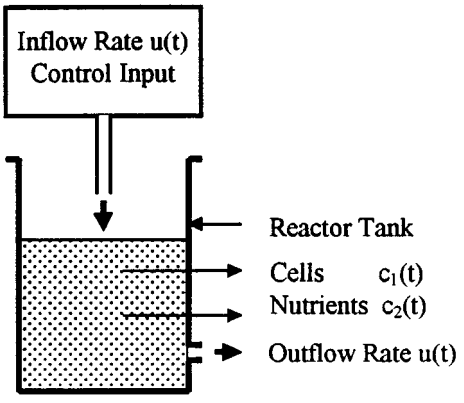

Figure 1. The Bioreactor tank and the process variables

at a rate equal to the incoming rate which is denoted by $u(t)$. This rate is called the flow rate and is the variable by which the bioreactor is controlled. The system therefore has only one control input, which is the externally supplied pure water. The bioreactor control problem is to maintain the cell concentration at a desired level.

The continuous-time equations of the plant dynamics are given by (1) and (2).

$$\dot{c}_1(t) = -c_1(t)u(t) + c_1(t)(1 - c_2(t))e^{c_2(t)/\gamma} \tag{1}$$

$$\dot{c}_2(t) = -c_2(t)u(t) + c_1(t)(1 - c_2(t))e^{c_2(t)/\gamma}\frac{1+\beta}{1+\beta-c_2(t)} \tag{2}$$

The state variables $c_1(t)$ and $c_2(t)$ can assume values between zero and one, the flow rate $u(t)$ can take values between zero and two. In the benchmark problem, the stable state of the process is defined to be $c_1 = 0{\cdot}1207$, $c_2 = 0{\cdot}8801$, and $u = 0{\cdot}7500$. The initial values of the state variables lie within $\pm$ 10% of the related stable state value and the initial value of each state variable is assumed to be uniformly distributed random variable over the above mentioned interval.

In the simulations, these equations are discretized by the use of first-order approximation with $\Delta = 0{\cdot}01$ s. In (1) and (2), $\beta = 0{\cdot}02$ (growth rate parameter), $\gamma = 0{\cdot}48$ (nutrient inhibition parameter). Controller inputs are the state variables and the command signal. The control interval is defined to be 50Δ, which means that the controller acquires the sensory information at integer multiples of 50Δ. The output of the controller is the flow rate $u(t)$. The objective is to achieve and maintain a desired cell concentration, by altering the flow rate.

The bioreactor is a challenging control problem for several reasons. Although the task involves few variables and is easily simulated, its nonlinearity makes it difficult to control. For example, small changes in the values of the parameters can cause the bioreactor to become unstable. The issues of delay, nonlinearity, instability and limit cycles can be studied with the bioreactor control problem. Additionally, significant delays exist between changes in flow rate and the response in cell concentration.[11] More detailed description of the problem can be found in the work of Ungar.[11]

Copyright © 1999 John Wiley & Sons, Ltd.

MODEL REFERENCE CONTROL OF A BIOREACTOR

Model reference control technique is applicable to wide variety of linear and nonlinear systems. The strategy evaluates some control inputs so that the plant output tracks a stable reference model output. There are two traditional approaches in the strategy, namely, direct adaptive control and indirect adaptive control. These approaches are illustrated in Figures 2 and 3.

Direct adaptive control scheme utilizes the instantaneous tracking error, which is denoted by e_c, in parameter updating. Several past control inputs and plant outputs are fed back to the controller by tapped delay lines, which are represented by TDL blocks in Figures 2 and 3. The parameters of the controller are directly adjusted to reduce some norm of the output error.[13]

Indirect adaptive control scheme employs an additional plant identification model which can provide information about the nonlinear components that appear in the actual plant dynamics.

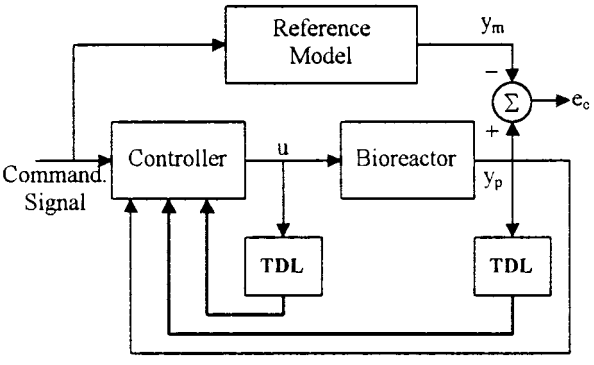

Figure 2. Direct control scheme

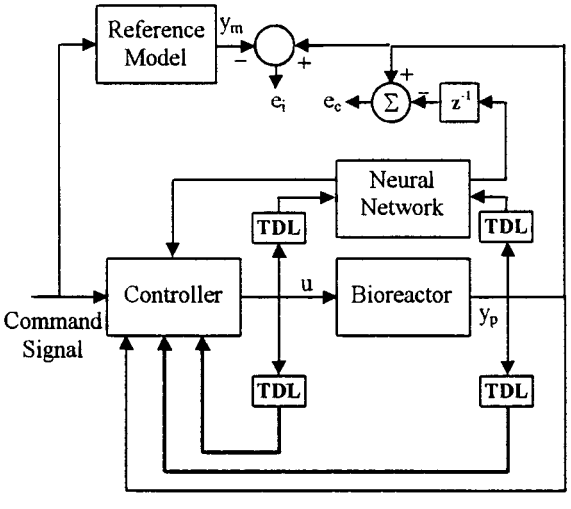

Figure 3. Indirect control scheme

Copyright © 1999 John Wiley & Sons, Ltd.

In this study, a feedforward neural network is used as the identifier. The identification can be carried out on-line or off-line. The strategy adopted by the authors is the indirect control scheme with off-line identification of the plant dynamics.

By introducing $f(c_1, c_2)$ and $g(c_2)$ and dropping the time variable, the governing equations of the bioreactor can be written more compactly as given by (3) and (4),

$$\dot{c}_1 = -c_1 u + f(c_1, c_2) \tag{3}$$

$$\dot{c}_2 = -c_2 u + f(c_1, c_2)\, g(c_2) \tag{4}$$

where,

$$f(c_1, c_2) = c_1 (1 - c_2)\, \mathrm{e}^{c_2/\gamma} \tag{5}$$

$$g(c_2) = \frac{1 + \beta}{1 + \beta - c_2} \tag{6}$$

Note that the system described by (3) and (4) is subject to the following compatibility condition:

$$\frac{f(c_1, c_2) - \dot{c}_1}{c_1} = \frac{f(c_1, c_2) g(c_2) - \dot{c}_2}{c_2} = u \tag{7}$$

One must notice that the left-hand side equality stipulates an obvious relation between c_1, c_2, $\dot{c}_1$, $\dot{c}_2$. For the system given by (3) and (4), a special reference model can be constructed with the following philosophy. Firstly the model output $c_{1\mathrm{m}}(t)$ must follow the command signal $r(t)$ (i.e. assuming that $c_{1\mathrm{m}}(t) = r(t)$ at the moment t_0, (8) is satisfied for all $t > t_0$).

$$\dot{c}_{1\mathrm{m}}(t) = -c_{1\mathrm{m}}(t) + r(t) \tag{8}$$

Secondly, since the system given by (3) and (4) satisfies the compatibility condition in (7), the model must satisfy this compatibility condition too. Otherwise, the range of the model output may assume some values that cannot be reached by the plant.

$$\frac{f(c_{1\mathrm{m}}, c_{2\mathrm{m}}) - \dot{c}_{1\mathrm{m}}}{c_{1\mathrm{m}}} = \frac{f(c_{1\mathrm{m}}, c_{2\mathrm{m}})\, g(c_{2\mathrm{m}}) - \dot{c}_{2\mathrm{m}}}{c_{2\mathrm{m}}} \tag{9}$$

Based on this philosophy, solving (9) for $\dot{c}_{2\mathrm{m}}(t)$, the $c_{2\mathrm{m}}(t)$ dynamics of the model can be formulated as follows:

$$\dot{c}_{2\mathrm{m}}(t) = f(c_{1\mathrm{m}}(t), c_{2\mathrm{m}}(t))\, g(c_{2\mathrm{m}}(t)) - \frac{c_{2\mathrm{m}}(t)}{c_{1\mathrm{m}}(t)} \left(f(c_{1\mathrm{m}}(t), c_{2\mathrm{m}}(t)) + c_{1\mathrm{m}}(t) \right) + \frac{c_{2\mathrm{m}}(t)}{c_{1\mathrm{m}}(t)} r(t) \tag{10}$$

Now the control input will be selected. The necessary inputs could be designed in such a way that (11) holds true.

$$c_{1\mathrm{m}}(t) = c_1(t) \quad \forall t \tag{11}$$

It must be emphasized that (11) is valid not only in the steady state but also in the transient period. This is under the assumption of identical plant-model initial conditions. This clearly implies (12) to hold true.

$$\dot{c}_{1\mathrm{m}}(t) = \dot{c}_1(t) \tag{12}$$

Copyright © 1999 John Wiley & Sons, Ltd.

Using this fact, the control signal can be formulated as described by (13).

$$u(c_1(t), c_2(t), r(t)) = 1 - \frac{r(t)}{c_1(t)} + \frac{f(c_1(t), c_2(t))}{c_1(t)} \tag{13}$$

However, with this control input, if we further require (14) to hold true under the identical plant-model initial conditions, (15) must hold true trivially.

$$c_{2\mathrm{m}}(t) = c_2(t) \quad \forall t \tag{14}$$

$$\dot{c}_{2\mathrm{m}}(t) = \dot{c}_2(t) \tag{15}$$

Hence the constraint in (16) in the state space is obtained.

$$g(c_2(t)) = \frac{1+\beta}{1+\beta-c_2(t)} = \frac{c_2(t)}{c_1(t)} \tag{16}$$

In the state space, implications of this constraint must be studied carefully. Equation (16) suggests the existence of an analytic relation between the state variables of both the bioreactor system and the reference model. The relation in (16) imposes the following two equalities:

$$c_{1\mathrm{m}} = \frac{1}{1+\beta} c_{2\mathrm{m}}(1+\beta-c_{2\mathrm{m}}) \tag{17}$$

$$c_{2\mathrm{m}} = \frac{1+\beta \pm \sqrt{(1+\beta)^2 - 4(1+\beta)c_{1\mathrm{m}}}}{2} \tag{18}$$

One directly infers from (18) that in order to have a real $(c_{1\mathrm{m}}, c_{2\mathrm{m}})$ pair, the discriminant must be nonnegative.

$$(1+\beta)^2 - 4(1+\beta)\, c_{1\mathrm{m}} \geqslant 0 \tag{19}$$

This is equivalent to the following;

$$c_{1\mathrm{m}} \leqslant \frac{1+\beta}{4} = 0{\cdot}255 \tag{20}$$

Equation (20) means that the applied command signal $r(t)$ must be less than or equal to 0·255. The second constraint, which is given next, is not so trivial. If (17) is differentiated to construct $c_{1\mathrm{m}}$ dynamics in (8) in terms of $c_{2\mathrm{m}}$ variable, one ends up with (21).

$$\dot{c}_{2\mathrm{m}} = \frac{c_{2\mathrm{m}}^2 - (1+\beta)c_{2\mathrm{m}} + (1+\beta)r}{(1+\beta) - 2c_{2\mathrm{m}}} \tag{21}$$

In order to have a non-zero denominator, $c_{2\mathrm{m}} \neq (1+\beta)/2$ must always be ensured. This is simply to modify (20) as follows:

$$c_{1\mathrm{m}} < 0{\cdot}255 \Leftrightarrow r < 0{\cdot}255 \tag{22}$$

Figure 4 illustrates the state dependency discussed above. For initial states close to AB curve, the state variables tend to lie on AB segment otherwise the tendency is towards BC segment of the trajectory. The shape of the trajectory followed depends on the command signal. An increasing

Copyright © 1999 John Wiley & Sons, Ltd.

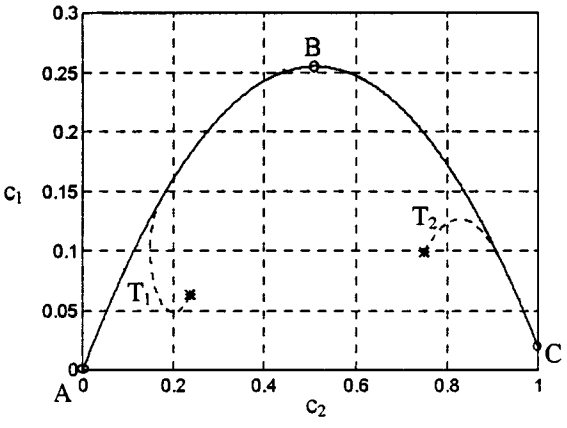

Figure 4. State dependency trajectory described by (31)

command signal may represent T_1-type trajectory while a decreasing command signal may result in T_2.

STABILITY ANALYSIS

In this section, the stability of the overall control system is explored. When the control, formulated in equation (13) is applied to the system, the stability conditions will be verified in the sense of Lyapunov.

Since the stability issue of the bioreactor control problem with model following property requires the analysis of the stability of a motion, the problem is transformed into an equivalent stability problem in which the tracking errors in cell and nutrient concentrations are considered as the parameters of the perturbation dynamics. Next, the stability of the origin of the perturbation dynamics is explained in detail.

$$e_1 = c_1 - c_{1\mathrm{m}} \tag{23}$$

$$e_2 = c_2 - c_{2\mathrm{m}} \tag{24}$$

$$V(e_1, e_2) = \tfrac{1}{2}(e_1^2 + e_2^2) \tag{25}$$

$V(e_1, \mathrm{e}_2)$ is positive definite for all $t > 0$.

$$\dot{V} = e_1\dot{e}_1 + e_2\dot{e}_2 \tag{26}$$

$$\dot{e}_1 = \dot{c}_1 - \dot{c}_{1\mathrm{m}} \tag{27}$$

$$\dot{e}_1 = -c_1u + f + c_{1\mathrm{m}} - r \tag{28}$$

$$\dot{e}_2 = \dot{c}_2 - \dot{c}_{2\mathrm{m}} \tag{29}$$

$$\dot{e}_2 = -c_2u + fg + c_{2\mathrm{m}} - gr \tag{30}$$

Copyright © 1999 John Wiley & Sons, Ltd.

In evaluating the expression in (30), the constraint in the state space (16) is utilized. By substituting the control u given by (13) into (28) and (30);

$$\dot{e}_1 = -f - c_1 + r + f + c_{1\mathrm{m}} - r \tag{31}$$

$$\dot{e}_1 = -(c_1 - c_{1\mathrm{m}}) = -e_1 \tag{32}$$

$$\dot{e}_2 = -\frac{c_2}{c_1} f - c_2 + \frac{c_2}{c_1} r + fg + c_{2\mathrm{m}} - gr \tag{33}$$

$$\dot{e}_2 = -(c_2 - c_{2\mathrm{m}}) = -e_2 \tag{34}$$

Using (32) and (34) in (26) yields the following;

$$\dot{V} = -(e_1^2 + e_2^2) \tag{35}$$

$$\dot{V} = -2V \tag{36}$$

Based on (25) and (36), the following three results hold true:

- $V(e_1, e_2)$ is positive definite
- $\mathrm{d}V/\mathrm{d}t$ is negative definite
- $V(e_1, e_2) \to \infty$ as $\|e\| \to \infty$

These results imply that the origin of the perturbation dynamics is globally asymptotically stable.

NEURAL NETWORKS AND PARTIAL IDENTIFICATION OF PROCESS DYNAMICS BY NEURO-IDENTIFIERS

A neural network architecture, in the sense of feedforward data processing, comprises three main parts. The first part is the input layer that distributes the input data to the processors in the next layer. The second part is comprised of the hidden layers where the nonlinear behaviour comes from. The third part is the output layer that transmits the response of the network to the real world. Input and output layers are directly accessible while the hidden layers are not. Each layer contains several number of processing elements that are generally called *neurons*. In Figure 5, the structure of a feedforward neural network is illustrated.

Neural networks can be used in the identification and control of nonlinear dynamical systems.[14,15]

$$J = \frac{1}{2} \sum_{p=1}^{P} \sum_{i=1}^{N} (d_i^p - y_i^p)^2 \tag{37}$$

For this purpose, the cost function given by (37) must be minimized. There are several ways of achieving the minimization of the function described by (37). For this purpose Backpropagation Training Algorithm,[15] which is the training methodology adopted in this paper, can be used. The choice of (37) is simply based on two facts: the cost function must represent the degree of similarity with minimal complexity and it must be differentiable with respect to the parameters of optimization. In (37), y_i^p denotes the ith entry of pth pattern in neural network response, d_i^p denotes the ith entry of pth target vector, P is the total number of training pairs contained in

Copyright © 1999 John Wiley & Sons, Ltd.

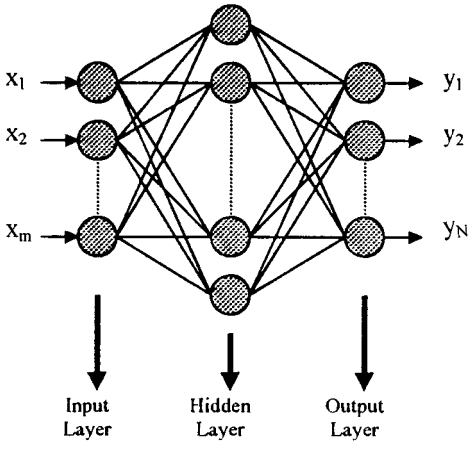

Figure 5. Feedforward neural network architecture

the training data set and N is the number of neural network outputs. Equations (38) and (39) describe the delta values for the output layer and hidden layer neurons, respectively.

$$\delta_j^{k+1,p} = (d_j^p - y_j^{k+1,p})\,\Psi'(S_j^{k+1,p}) \tag{38}$$

$$\delta_j^{k+1,p} = \left(\sum_{h=1}^{\#\,\text{neurons}_{k+2}} \delta_h^{k+2,p}\, w_{jh}^{k+1} \right) \Psi'(S_j^{k+1,p}) \tag{39}$$

In (38) and (39), S_j denotes the net summation of the jth neuron in the $(k+1)$th layer, Ψ is the nonlinear activation function attached to each neuron in the hidden layer. Having evaluated the delta values during the backward pass, the weight update rule given in (40) is applied for each training pair.

$$\Delta w_{ij}^k = \eta \delta_j^{k+1,p}\, o_i^{k,p} \tag{40}$$

The neural network structure imitating the bioreactor dynamics for the partial identification scheme is illustrated in Figure 6. The reason why the term *partial identification* used is the fact that, only the value of the function $f(c_1, c_2)$ that appears in the bioreactor dynamics is needed. In order to construct the control to be applied, the state variables need to be observed and the function $f(c_1, c_2)$ needs to be estimated.

In Figure 6, y_1 and y_2 realize the first and the second terms in (1), respectively, y_3 and y_4 perform the same for (2). The bias values of the linear output neurons are set to previous state values so that the first order discretization of the governing equations is achieved through the use of a neural network.

ERROR CONVERGENCE ANALYSIS

In this section, it is proven that the tracking errors between the reference model outputs and the actual plant outputs tend to zero in the limiting case. If $f(c_1, c_2)$ is estimated by a neural network,

Copyright © 1999 John Wiley & Sons, Ltd.

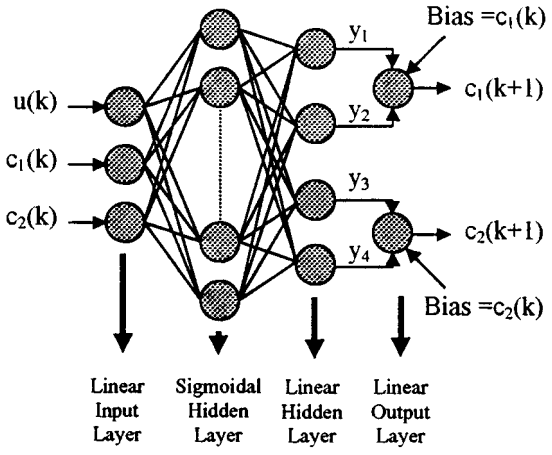

Figure 6. Partial identification of the Bioreactor dynamics

then, (13) becomes,

$$u = \frac{\hat{f}(c_1, c_2) + c_1 - r}{c_1} \tag{41}$$

If this control is written into (3) and (4); (42) and (43) are found.

$$\dot{c}_1 = -c_1 + (f(c_1, c_2) - \hat{f}(c_1, c_2)) + r \tag{42}$$

$$\dot{c}_2 = -c_2 + g(c_2)r - \frac{g(c_2)}{f(c_1, c_2)}(f(c_1, c_2) - \hat{f}(c_1, c_2)) \tag{43}$$

From the approximation theorems given in Hornik[16] and Funahashi,[17] the function $f(c_1, c_2)$ can be realized by neural networks such that the approximation error in the neural network output remains within a prespecified level. As long as a neural network realizes the function $f(c_1, c_2)$ precisely, the difference between the network output and the actual value of the function is negligible. This difference is called realization error and is denoted by $\varepsilon(t)$. For the full analysis, which requires that $\varepsilon(t)$ is not neglected, the error dynamics forced by this term can be formulated as given by (44) and (45).

$$\dot{c}_{1m} - \dot{c}_1 = -(c_{1m} - c_1) - \varepsilon(t) \tag{44}$$

$$\dot{c}_{2m} - \dot{c}_2 = -(c_{2m} - c_2) - \frac{g(c_2)}{f(c_1, c_2)}\varepsilon(t) \tag{45}$$

Or equivalently,

$$\dot{e}_1 = -e_1 - \varepsilon(t) \tag{46}$$

$$\dot{e}_2 = -e_2 - \frac{g(c_2)}{f(c_1, c_2)}\varepsilon(t) \tag{47}$$

Copyright © 1999 John Wiley & Sons, Ltd.

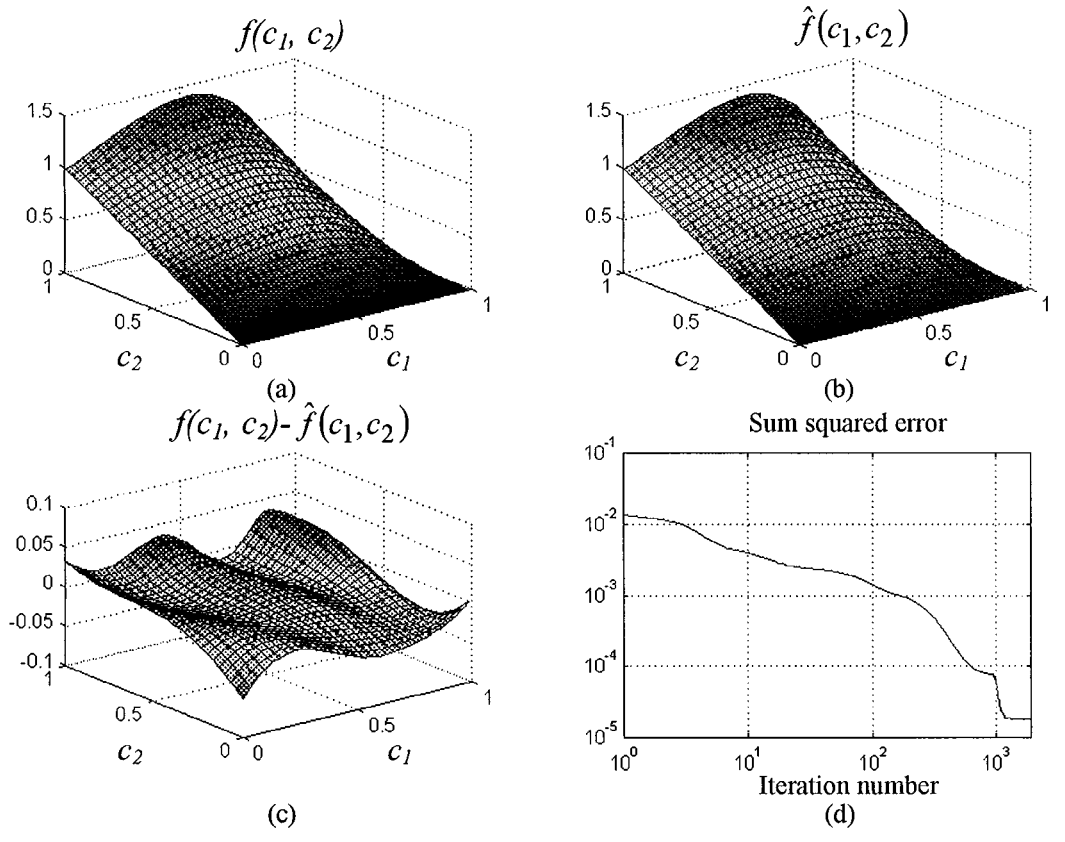

Figure 7. (a) Actual f function (b) Estimated f function (c) Discrepancy between actual and estimated f functions (d) Sum squared error versus iteration number

Equations (46) and (47) reveal that the error dynamics is stable, moreover, the error in c_1 is forced to track $\varepsilon(t)$ and the error in c_2 is forced to track $(g/f)\varepsilon(t)$. This clearly stipulates that the tracking performance of the control system strictly depends on the accuracy of the mapping performed by the neuroidentifier. The better approximation leads to the better tracking performance. In the top row of Figure 7, the actual and estimated values of the function f are illustrated. In the bottom left plot of Figure 7, the discrepancy between the actual and estimated values, which is denoted by ε throughout the text, is shown. The bottom right plot demonstrates the sum-squared error versus iteration number. In fact, this is the value of cost defined by (37).

SIMULATION RESULTS

The feasibility and the efficacy of the novel approach described in the previous sections have been demonstrated by a series of simulations. It is seen that the algorithm results in a stable control of the bioreactor. The plant outputs follow that of the reference model quite closely. Two sets of simulation study results are given below. The first set considers the case of a sinusoidal reference

Copyright © 1999 John Wiley & Sons, Ltd.

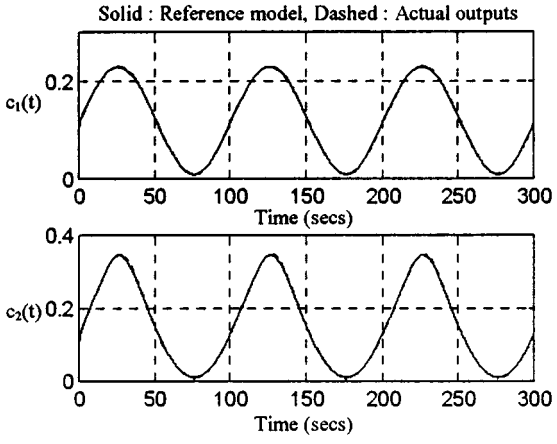

Figure 8. Cell and nutrient concentration graphs for the reference model and for the actual plant. Command signal is $r(t) = 0{\cdot}12 + 0{\cdot}11\sin(2\pi t/100)$

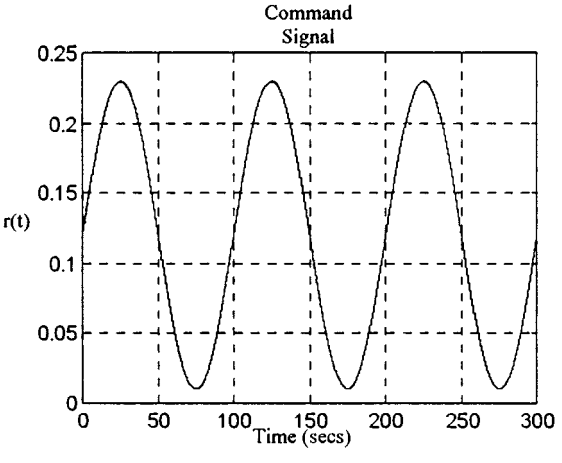

Figure 9. Command signal graph

signal. When choosing the upper bound of this command signal, the constraint given by (22) must be kept in mind. Otherwise, the system outputs will not track the reference model outputs. In Figure 8, the time variation of the cell and the nutrient concentrations are given both for the reference model and the actual plant. The plant follows the model quite closely for the command signal shown in Figure 9. The state tracking errors are depicted in Figure 10. The control signal that is applied to the plant is illustrated in Figure 11.

Figures 12–15 illustrate similar simulation results for a pulse train type of command signal. The reason for this choice is to demonstrate the model following capability of the control system in the case of abrupt changes in the command signal. As can be inferred from Figure 14, the

Copyright © 1999 John Wiley & Sons, Ltd.

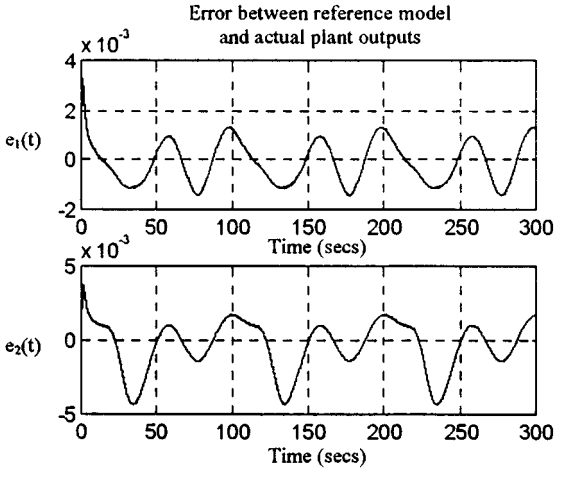

Figure 10. Error graph for the cell and nutrient concentration

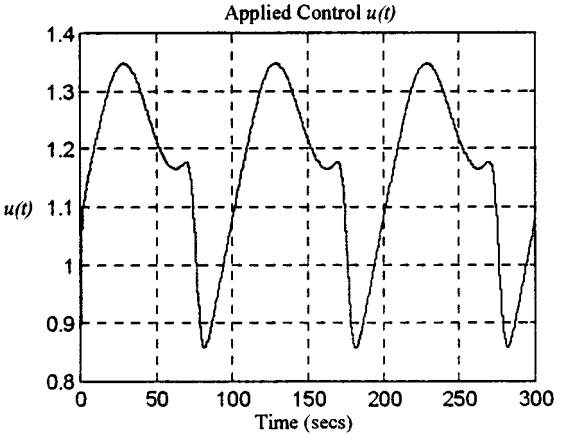

Figure 11. Applied control signal

performance of the controller is satisfactory in the sense that when the command signal comprises sharp changes, the model following property is preserved.

In Figures 10 and 14, tracking errors are illustrated. The reason why there are such errors is directly relevant to the performance of neural estimator. Since the function to be realized is a continuous function, and, since a finite number of training samples can be of interest, there will always be such tracking errors stemming from the neural approximation errors. The perfect tracking is observed when the original $f(c_1, c_2)$ function used with the condition that the initial values of the state variables for both the reference model and the actual plant are equal to each other.

Copyright © 1999 John Wiley & Sons, Ltd.

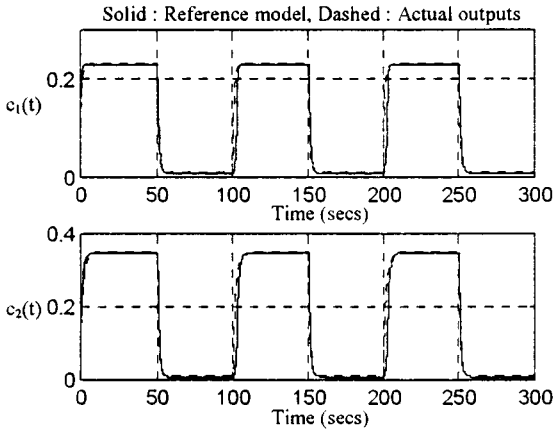

Figure 12. Cell and nutrient concentration graphs for the reference model and for the actual plant. Command signal is $r(t) = 0{\cdot}12 + 0{\cdot}11\mathrm{sgn}(\sin(2\pi t/100))$

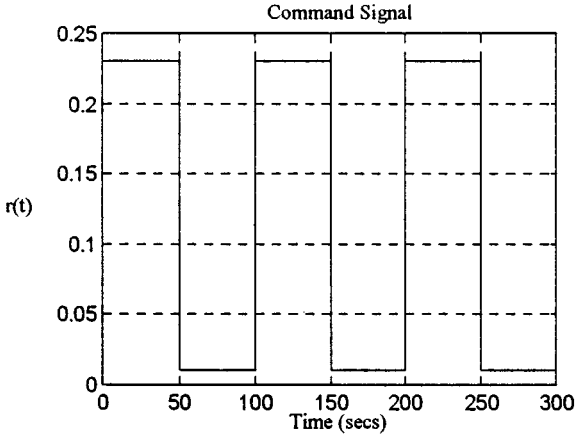

Figure 13. Command signal graph

In the simulation results presented, the neuroidentifier has three inputs reserved for system states and the applied control. The outputs of the identifier are the estimates of the next states. Two hidden layers are used, the first one has eight neurons each possessing tan-sigmoidal neuron nonlinearities, and the second hidden layer comprises four linear neurons. Since the input variables of neuroidentifier assume admissible values for such a neural network application, no preprocessing or normalization is needed. If the variables involved assume too large or too small magnitudes, heuristically, these are mapped onto an interval, which is typically bounded by plus and minus unity, so that the learning performance is increased. The training is continued until the sum-squared error decreases to 18e-6 for the randomly generated training data set, which contains 500 samples from $0 < c_1 < 1$, $0 < c_2 < 1$ and $0 < u < 2$. Training procedure takes 45 s

Copyright © 1999 John Wiley & Sons, Ltd.

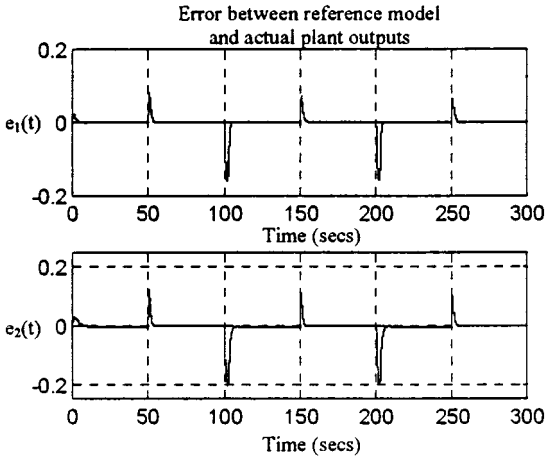

Figure 14. Error graph for the cell and nutrient concentration

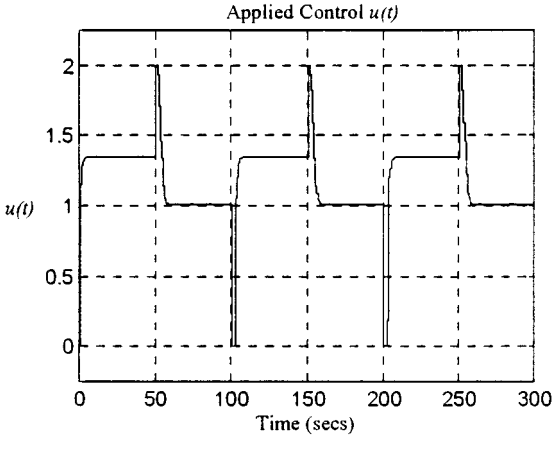

Figure 15. Applied control signal

on a Pentium II 266 PC with trainer coded in Borland C environment. The square of the least value seen in the bottom right plot of Figure 7 and the minimal value in the bottom left plot might cause confusion. This occurs due to the use of different data sets in training phase (with randomly generated data) and visualization phase (with grid data). This is a well-known phenomenon in the neural network terminology. If the set used in training had been shown as surface points, the square of the least value seen in the upper plots would be the same as what is visualized in the lower plots. This fact is attributed to the generalization property of neural networks.

Copyright © 1999 John Wiley & Sons, Ltd.

CONCLUSIONS

In this paper, a special nonlinear controller for the bioreactor benchmark problem is formulated. The approach is based on Model Reference Control theory. A stable reference model has been chosen and the philosophy that lies behind this choice is explained. The analysis and the design methodology stipulate that the controller is a static function of system variables and the command signal. It is shown that the controller itself is stable in the sense of bounded inputs/bounded outputs criterion as well as it is locally stabilizing the overall control system in the sense of Lyapunov. Simulation results illustrate that the proposed approach is a good candidate for the control of bioreactors. Two different types of command signals are used to demonstrate the capability of the model following property. In the first trial, a sinusoidal, in the second trial, a pulse train is applied as the command signal. Since the applicable control signal is bounded by 2·0, in the cases where the changes in reference model output are large in magnitude, larger controls are evaluated by the controller, but these are saturated at the upper bound. The simulation results have revealed that if the command signal approaches to 0·255, the control signal is likely to saturate.

The approach described in this paper requires *a priori* knowledge about the governing equations of the bioreactor dynamics. Future study aims to realize nonlinear controllers utilizing on-line learning methodologies that need less *a priori* information about plant dynamics and environment.

ACKNOWLEDGEMENTS

This work is supported in part by a grant of Foundation for Promotion of Advanced Automation Technology and Bogazici University Research Fund, Project no: 97A0202.

REFERENCES

1. Anderson, C. W. and W. T. Miller III, 'Challenging control problems', in *Neural Networks for Control*, W. T. Miller III, R. S. Sutton, and P. J. Werbos (Eds), MIT Press, Cambridge, MA, 1990, pp. 475–510.
2. Agrawal, P. and H. C. Lim, 'Analysis of various control schemes for continuopus bioreactors', in *Advances in Biochemical Engineering & Biotechnology*, A. Fiechter (Ed), Vol. 30, Springer, New York, 1984, pp. 61–90.
3. Bastin, G. and D. Dochain, *On-Line Estimation and Adaptive Control of Bioreactors*, Elesevier, New York, 1990.
4. Zhao, Y. and S. Skogestad, 'Comparison of various control configurations for continuous bioreactors', *Ind. Engng. Chem. Res.*, **36**, 697–705 (1997).
5. Passino, K. M., 'Intelligent control for autonomous systems', *IEEE Spectrum*, **32**, 55–62 (1996).
6. Linkens, D. A. and H. O. Nyongesa, 'Learning systems in intelligent control: an appraisal of fuzzy, neural and genetic algorithm control applications', *IEE Proc. Control Theory Appl.*, **143**, 367–386 (1996).
7. Aoyama, A., F. J. Doyle III and V. Venkatasubramanian, 'Control-affine neural network approach for non-minimum-phase nonlinear process control', *J. Process Control*, **6**, 17–26 (1996).
8. Bersini H. and V. Gorrini, 'A simplification of the backpropagation-through-time algorithm for optimal neurocontrol', *IEEE Trans. Neural Networks*, **8**, 437–441 (1997).
9. Zitar, R. A. and M. H. Hassoun, 'Neurocontrollers trained with rules extracted by genetic assisted reinforcement learning system', *IEEE Trans. Neural Networks*, **6**, 859–879 (1995).
10. Feldkamp L. A. and G. V. Puskorius, 'Neural network approaches to process control', *Proc. WCNN 93 Portland: World Congress on Neural Networks*, 11–15 July 1993, Oregon, 1993 Vol. 1, pp. I-451–I-456.
11. Ungar, L. H., 'A bioreactor benchmark for adaptive-network based process control', in *Neural Networks for Control*, W. T. Miller III, R. S. Sutton, P. J. Werbos (Eds), MIT Press, Cambridge, MA, 1990, pp. 387–402.
12. Gorinevsky, D, 'Sampled-data indirect adaptive control of bioreactor using affine radial basis function network architecture', *Trans. ASME, J. Dyn. System Control*, **119**, 94–96 (1997).

Copyright © 1999 John Wiley & Sons, Ltd.

13. Narendra, K. S., Parthasarathy, K., 'Identification and control of dynamical systems using neural networks', *IEEE Trans. Neural Networks*, **1**, 4–27 (1990).
14. Efe, M. O., Identification and control of nonlinear dynamical systems using neural networks, M.S. Thesis, Bogazici University, 1996.
15. Jang, J.-S. R. and C.-T. Sun, 'Neuro-fuzzy modelling and control', *Proc. IEEE*, **83**, 378–406 (1995).
16. Hornik, K., 'Multilayer feedforward networks are universal approximators', *Neural Networks*, **2**, 359–366 (1989).
17. Funahashi, K., 'On the approximate realization of continuous mappings by neural networks', *Neural Networks*, **2**, 183–192 (1989).

Copyright © 1999 John Wiley & Sons, Ltd.